Article

Oxidation Mechanism of Phenols by Dicopper–Dioxygen (Cu/O) Complexes

Takao Osako, Kei Ohkubo, Masayasu Taki, Yoshimitsu Tachi, Shunichi Fukuzumi, and Shinobu Itoh

J. Am. Chem. Soc., **2003**, 125 (36), 11027-11033• DOI: 10.1021/ja029380+ • Publication Date (Web): 16 August 2003

J|A|C|S
ARTICLES
Published on Web 08/16/2003

Oxidation Mechanism of Phenols by Dicopper−Dioxygen (Cu_2/O_2) Complexes

Takao Osako,[†] Kei Ohkubo,[‡] Masayasu Taki,[†] Yoshimitsu Tachi,[†] Shunichi Fukuzumi,*[,‡] and Shinobu Itoh*[,†]

Contribution from the Department of Chemistry, Graduate School of Science, Osaka City University, 3−3−138 Sugimoto, Sumiyoshi-ku, Osaka 558-8585, Japan, and Department of Material and Life Science, Graduate School of Engineering, Osaka University, CREST, Japan Science and Technology Corporation, 2−1 Yamada-oka, Suita, Osaka 565-0871, Japan

Received November 18, 2002; E-mail: fukuzumi@chem.eng.osaka-u.ac.jp; shinobu@sci.osaka-cu.ac.jp

Abstract: The first systematic studies on the oxidation of neutral phenols (ArOH) by the (μ-η^2:η^2-peroxo)-dicopper(II) complex (**A**) and the bis(μ-oxo)dicopper(III) complex (**B**) supported by the 2-(2-pyridyl)ethylamine tridentate and didentate ligands L^{Py2} and L^{Py1}, respectively, have been carried out in order to get insight into the phenolic O−H bond activation mechanism by metal-oxo species. In both cases (**A** and **B**), the C−C coupling dimer was obtained as a solely isolable product in ∼50% yield base on the dicopper−dioxygen (Cu_2/O_2) complexes, suggesting that both **A** and **B** act as electron-transfer oxidants for the phenol oxidation. The rate-dependence in the oxidation of phenols by the Cu_2/O_2 complexes on the one-electron oxidation potentials of the phenol substrates as well as the kinetic deuterium isotope effects obtained using ArOD have indicated that the reaction involves a proton-coupled electron transfer (PCET) mechanism. The reactivity of phenols for net hydrogen atom transfer reactions to cumylperoxyl radical (**C**) has also been investigated to demonstrate that the rate-dependence of the reaction on the one-electron oxidation potentials of the phenols is significantly smaller than that of the reaction with the Cu_2O_2 complexes, indicative of the direct hydrogen atom transfer mechanism (HAT). Thus, the results unambiguously confirmed that the oxidation of phenols by the Cu_2O_2 complex proceeds via the PCET mechanism rather than the HAT mechanism involved in the cumylperoxyl radical system. The reactivity difference between **A** and **B** has also been discussed by taking account of the existed fast equilibrium between **A** and **B**.

Introduction

Copper-catalyzed oxidation of phenols by dioxygen has been studied extensively in order to elucidate the catalytic mechanism of copper oxidases and copper monooxygenases as well as to develop an efficient catalyst for regioselective polymerization of phenols to poly(1,4-phenylene oxide) (PPO).[1−3] In particular, much recent attention has been focused on the reactions of phenols with two distinct dicopper−dioxygen (Cu_2/O_2) complexes, (μ-η^2:η^2-peroxo)dicopper(II) complex and bis(μ-oxo)-dicopper(III) complex (**A** and **B** in Chart 1, respectively), to understand the mechanism of phenolase activity of tyrosinase.[4−8]

Chart 1

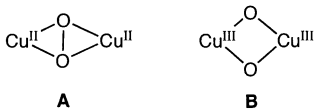

A **B**

In this context, we have recently demonstrated that the (μ-η^2:η^2-peroxo)dicopper(II) complex (**A**) oxidizes lithium salts of phenols to the corresponding catechols via an *electrophilic aromatic substitution mechanism* in an association complex between the phenolate and the peroxo complex (Scheme

* To whom correspondence should be addressed.
[†] Osaka City University.
[‡] Osaka University, CREST, Japan Science and Technology Corporation.

(1) (a) Casella, L.; Monzani, E.; Gullotti, M.; Cavagnino, D.; Cerina, G.; Santagostini, L.; Ugo, R. *Inorg. Chem.* **1996**, *35*, 7516−7525. (b) Réglier, M.; Jorand, C.; Waegell, B. *J. Chem. Soc., Chem. Commun.* **1990**, 1752−1755. (c) Sayre, L. M.; Nadkarni, D. V. *J. Am. Chem. Soc.* **1994**, *116*, 3157−3158.
(2) (a) Iwata, M.; Emoto, S. *Tetrahedron Lett.* **1974**, 759−760. (b) Capdevielle, P.; Maumy, M. *Tetrahedron Lett.* **1982**, *23*, 1573−1576. (c) Chioccara, F.; Di Gennaro, P.; La Monica, G.; Sebastiano, R.; Rindone, B. *Tetrahedron* **1991**, *47*, 4429−4434.
(3) (a) Higashimura, H.; Fujisawa, K.; Moro-oka, Y.; Kubota, M.; Shiga, A.; Terahara, A.; Uyama, H.; Kobayashi, S. *J. Am. Chem. Soc.* **1998**, *120*, 8529−8530. (b) Higashimura, H.; Kubota, M.; Shiga, A.; Fujisawa, K.; Moro-oka, Y.; Uyama, H.; Kobayashi, S. *Macromolecules* **2000**, *33*, 1986−1995.
(4) Kitajima, N.; Koda, T.; Iwata, Y.; Moro-oka, Y. *J. Am. Chem. Soc.* **1990**, *112*, 8833−8839.
(5) (a) Paul, P. P.; Tyeklár, Z.; Jacobson, R. R.; Karlin, K. D. *J. Am. Chem. Soc.* **1991**, *113*, 5322−5332. (b) Obias, H. V.; Lin, Y.; Murthy, N. N.; Pidcock, E.; Solomon, E. I.; Ralle, M.; Blackburn, N. J.; Neuhold, Y.-M.; Zuberbühler, A. D.; Karlin, K. D. *J. Am. Chem. Soc.* **1998**, *120*, 12960−12961.
(6) (a) Mahapatra, S.; Halfen, J. A.; Wilkinson, E. C.; Que, L., Jr.; Tolman, W. B. *J. Am. Chem. Soc.* **1994**, *116*, 9785−9786. (b) Halfen, J. A.; Young, V. G., Jr.; Tolman, W. B. *Inorg. Chem.* **1998**, *37*, 2102−2103.
(7) (a) Mahadevan, V.; DuBois, J. L.; Hedman, B.; Hodgson, K. O.; Stack, T. D. P. *J. Am. Chem. Soc.* **1999**, *121*, 5583−5584. (b) Mahadevan, V.; Henson, M. J.; Solomon, E. I.; Stack, T. D. P. *J. Am. Chem. Soc.* **2000**, *122*, 10249−10250. (c) Mirica, L. M.; Vance, M.; Rudd, D. J.; Hedman, B.; Hodgson, K. O.; Solomon, E. I.; Stack, T. D. P. *J. Am. Chem. Soc.* **2002**, *124*, 9332−9333.
(8) Santagostini, L.; Gullotti, M.; Monzani, E.; Casella, L.; Dillinger, R.; Tuczek, F. *Chem. Eur. J.* **2000**, *6*, 519−522.

Scheme 1

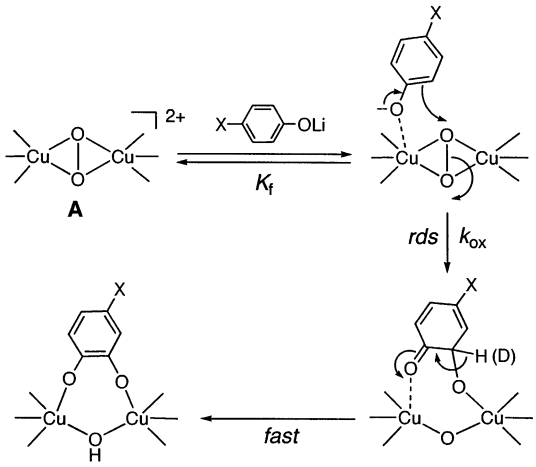

1), providing significant mechanistic insights into the enzymatic reaction.[9] In this case, neither the *o*-quinone nor the C−C coupling dimer of phenol was obtained, being in sharp contrast to the oxidation of neutral phenols by the peroxo and bis(μ-oxo) complexes under similar reaction conditions, where the C−C coupling dimer was the major product.[5−7] The dimer formation unambiguously indicates the formation of phenoxyl radical intermediates in the reaction of neutral phenols. Then, an important question arises; what is the major factor controlling the reaction pathways between the catechol formation (oxygenation) and the C−C coupling reaction (phenoxyl radical formation)?

Conversion of a phenol to a phenoxyl radical is an important process in a variety of biological systems. Particular attention has recently focused on the catalytic roles of phenoxyl radical intermediates in ribonucleotide reductases, cytochrome *c* oxidase, prostaglandin H synthase, and photosystem II.[10] The phenoxyl radicals in those systems are derived from the active site tyrosines via the oxidation with transition-metal oxo species in the respective enzymes. Thus, the mechanism of phenoxyl radical formation in the reaction with transition-metal oxo complexes is also an important subject in bioinorganic chemistry. For the formation of a phenoxyl radical species from a neutral phenol, there are two possible reaction pathways: direct hydrogen atom transfer (HAT) and proton-coupled electron transfer (PCET). Mechanistic arguments concerning the net hydrogen atom transfer reaction (HAT vs PCET) is one of the most important and fundamental issues in several biological and industrial processes involving O−H and C−H bond activation.[10−12]

We report herein the first systematic study on the oxidation of neutral phenols (ArOH) by the (μ-η^2:η^2-peroxo)dicopper(II) complex (**A**) and the bis(μ-oxo)dicopper(III) complex (**B**) supported by 2-(2-pyridyl)ethylamine tridentate and didentate ligands L^{Py2} and L^{Py1}, respectively (Chart 2).[9,13] Comparison of the rate-dependences in the oxidation of phenols by the Cu_2/O_2 complexes on the one-electron oxidation potentials of the phenol substrates (E^0_{ox}) provides profound insights into the mechanistic basis of the phenol-oxidation as well as the electron-transfer oxidation ability of the Cu_2/O_2 complexes. We have also examined the reactivity of phenols for hydrogen atom transfer reaction using cumylperoxyl radical (**C**) as the hydrogen acceptor. The rates of hydrogen atom transfer from phenols to cumylperoxyl radical were determined directly by monitoring the decay of cumylperoxyl radical by ESR. Direct comparison of the rate-dependence on E^0_{ox} of phenols between the Cu_2/O_2 system and the cumylperoxyl radical system provided a quantitative basis to compare the PCET mechanism and the HAT mechanism.

Chart 2

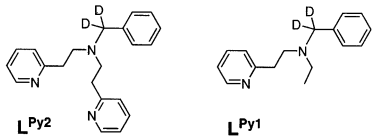

Since Tolman et al. discovered the peroxo/bis(μ-oxo) equilibrium, the factors to control which isomeric core in the Cu_2/O_2 complexes predominates have been extensively studied.[7b,c,14−18] However, quantitative comparison of the oxidation ability of these two isomeric cores (**A** and **B**) in Cu_2/O_2 intermediates is quite difficult in general due to the existed fast equilibrium between **A** and **B**.[19] The fast equilibration between the two species always makes it difficult to conclude which is the real active oxygen species in the oxidation reactions of Cu_2/O_2 complexes. In this study, this issue in the oxidation of phenols by the Cu_2/O_2 complexes has also been discussed based on the experimental data of kinetics and product analysis.

Experimental Section

General. All chemicals used in this study, except the ligands, deuterated para-substituted phenols, and the copper(I) complexes, were commercial products of the highest available purity and were further purified by the standard methods, if necessary.[20] Synthetic procedures of the ligands and the copper(I) complexes as well as the lithium phenolates were reported previously.[9,13] The deuterated phenols (*p*-X-C_6H_4OD) were prepared by the reaction of the lithium phenolates with acetic acid-*d* CH_3COOD (98%, Aldrich), and the purity of the product was confirmed by ^1H NMR and MS. FT-IR spectra were recorded with a Shimadzu FTIR-8200PC. UV−vis spectra were measured using a Hewlett-Packard HP8453 diode array spectrophotometer with a Unisoku thermostated cell holder designed for low-temperature measurements. Mass spectra were recorded with a JEOL JMS-700T Tandem MS station, and the GC-MS analyses were carried out by using a Shimadzu GCMS-QP2000 gas chromatograph mass spectrometer. ^1H and ^{13}C NMR spectra were recorded on a JEOL FT-NMR Lambda 300WB or a JEOL FT-NMR GX-400 spectrometer. ESR measurements were performed on a JEOL X-band spectrometer (JES-ME-LX).

(9) Itoh, S.; Kumei, H.; Taki, M.; Nagatomo, S.; Kitagawa, T.; Fukuzumi, S. *J. Am. Chem. Soc.* **2001**, *123*, 6708−6709.
(10) Stubbe, J.; van der Donk, W. A. *Chem. Rev.* **1998**, *98*, 705−762.
(11) (a) Mayer, J. M. *Acc. Chem. Rev.* **1998**, *31*, 441−450. (b) Roth, J. P.; Yoder, J. C.; Won, T.-J.; Mayer, J. M. *Science* **2001**, *294*, 2524−2526.
(12) Cukier, R. I.; Nocera, D. G. *Annu. Rev. Phys. Chem.* **1998**, *49*, 337−369.
(13) Taki, M.; Itoh, S.; Fukuzumi, S. *J. Am. Chem. Soc.* **2001**, *123*, 6203−6204.
(14) Halfen, J. A.; Mahapatra, S.; Wilkinson, E. C.; Kaderli, S.; Young, V. G., Jr.; Que, L., Jr.; Zuberbühler, A. D.; Tolman, W. B. *Science* **1996**, *271*, 1397−1400.
(15) Tolman, W. B. *Acc. Chem. Res.* **1997**, *30*, 227−237.
(16) Que, L., Jr.; Tolman, W. B. *Angew. Chem., Int. Ed.* **2002**, *41*, 1114−1137.
(17) (a) Taki, M.; Teramae, S.; Nagatomo, S.; Tachi, Y.; Kitagawa, T.; Itoh, S.; Fukuzumi, S. *J. Am. Chem. Soc.* **2002**, *124*, 6367−6377. (b) Itoh, S.; Fukuzumi, S. *Bull. Chem. Soc. Jpn.* **2002**, *75*, 2081−2095.
(18) Liang, H.-C.; Zhang, C. X.; Henson, M. J.; Sommer, R. D.; Hatwell, K. R.; Kaderli, S.; Zuberbühler, A. D.; Rheingold, A. L.; Solomon, E. I.; Karlin, K. D. *J. Am. Chem. Soc.* **2002**, *124*, 4170−4171.
(19) Stack and co-workers reported that the equilibrium between the peroxo complex (**A**) and the bis(μ-oxo) complex (**B**) supported by *N*,*N*′-di-*tert*-butyl-*N*,*N*′-dimethylethylenediamine ligand was relatively slow in 2-MeTHF.[7b] The slow equilibration allowed them to examine the reactivity difference between **A** and **B** toward 2,4-di-*tert*-butylphenol and PPh_3.[7b]
(20) Perrin, D. D.; Armarego, W. L. F.; Perrin, D. R. *Purification of Laboratory Chemicals*, 4th ed.; Pergamon Press: Elmsford, NY, 1996.

Product Analysis. The (μ-η^2:η^2-peroxo)dicopper(II) complex and the bis(μ-oxo)dicopper(III) complex supported by L^{Py2} and L^{Py1}, respectively, were generated in situ by treating the corresponding copper(I) complex $[Cu^I(L)]PF_6$ (0.04 mmol) with O_2 gas at −80 °C in anhydrous acetone (50 mL) for 10−20 min. Excess O_2 was then removed by bubbling Ar gas into the solution for 10 min. A cold solution (−80 °C) of phenol (0.08 mmol) in 5 mL of anhydrous acetone was added into the solution by cannulation, and the mixture was stirred for overnight at this temperature using an EYELA low-temp pair-stirrer PSL-1800. The reaction was quenched by adding 0.4 M $HClO_4$ (5 mL) at −80 °C, and then the mixture was warmed to room temperature. After evaporation of the solvent, the remaining residue was extracted by ethyl acetate (5 mL × 3), and the combined ethyl acetate solution was dried over $MgSO_4$. After removal of $MgSO_4$ by filtration, concentration of the solvent gave an organic material. Formation of the C−C coupling dimer products was confirmed by GC-MS and ^{1}H NMR, and the yields were determined by ^{1}H NMR using CH_2ClCH_2Cl as an internal reference.

Electrochemical Measurements. The second harmonic ac voltammetry (SHACV) was employed to determine the one-electron oxidation potentials (E^0_{ox}) of phenols. The SHACV measurements were performed using an ALS-630A electrochemical analyzer in deaerated CH_3CN containing 0.10 M $Bu_4N^+PF_6^-$ as a supporting electrolyte. The platinum working electrode was polished with alumina suspension and rinsed with CH_3CN before use. The counter electrode was a platinum wire. The measured potentials were recorded with respect to an $Ag/AgNO_3$ (0.01 M) reference electrode. The E^0_{ox} values (vs $Ag/AgNO_3$) were converted to those vs SCE by addition of 0.29 V. All electrochemical measurement were carried out at 25 °C under an atmospheric pressure of Ar in a glovebox (Miwa Co. Ltd.)

Kinetic Measurements by UV−vis. The copper−dioxygen complexes (**A** and **B**) were generated in situ by the reaction of the Cu^I complexes (0.15 mM) and dry O_2 gas in acetone at −80 °C (introduced by gentle bubbling for a few minutes) in a UV−vis cell (1 cm path length), which was held in a Unisoku thermostated cell holder designed for the low-temperature experiments (fixed within ±0.5 °C). After formation of the dicopper−dioxygen complexes, excess O_2 was removed by bubbling Ar into the solution for 5 min. Then, the reaction was initiated by adding an excess amount of the substrate into the solution, and the pseudo-first-order rate constants (k_{obs}) were determined by following the decrease in the absorption due to the dicopper−oxygen complexes.

Kinetic Measurements by ESR. Typically, photoirradiation of an oxygen-saturated propionitrile solution containing di-*tert*-butyl peroxide (1.0 M) and cumene (1.0 M) with a 1000 W Mercury lamp resulted in formation of cumylperoxyl radical ($g = 2.0156$) which could be detected at −80 °C. The g value was calibrated by using an Mn^{2+} marker. Upon cutting off the light, the decay of the ESR intensity was recorded with time. The decay rate was accelerated by the presence of ArOH (1.0×10^{-2} M). Rates of hydrogen atom transfer from ArOH to cumylperoxyl radical were monitored by measuring the decay of ESR signal in the presence of various concentrations of ArOH in acetone at −80 °C. Pseudo-first-order rate constants were determined by a least-squares curve fit using a microcomputer. The first-order plots of $\ln(I - I_\infty)$ vs time (I and I_∞ are the ESR intensity at time t and the final intensity, respectively) were linear for three or more half-lives with the correlation coefficient, $r > 0.99$.

Results and Discussion

Oxidation of Phenols by the (μ-η^2:η^2-Peroxo)dicopper(II) Complex (A). The (μ-η^2:η^2-peroxo)dicopper(II) complex (**A**) was generated by the reaction of the copper(I) complex of L^{Py2} with dioxygen at −80 °C in acetone as previously reported.[9] Treatment of 4-substituted phenols such as *p*-$MeOC_6H_4OH$ (**1**), *p*-$Bu^tC_6H_4OH$ (**5**), and *p*-ClC_6H_4OH (**10**) (for the numbering of phenol substrates, see Table 1) with the peroxo complex **A** (0.02 mmol) at −80 °C under anaerobic conditions gave the corresponding C−C coupling dimer in 42%, 38%, and 32% yields, respectively, based on the peroxo complex **A**. The lower yields for **5** and **10** can be attributed to their lower reactivity toward the peroxo complex **A**. Namely, the oxidation of **5** and **10** by **A** competes with the self-decomposition of **A**. Then, the nearly 50% yield of the dimer product based on **A** suggests that the (μ-η^2:η^2-peroxo)dicopper(II) complex formally acts as an one-electron oxidant for ArOH producing an equimolar amount of ArO$^\bullet$ (0.02 mmol), which spontaneously dimerizes to give the C−C coupling product in nearly 50% yield (0.01 mmol) based on **A**.[21]

Table 1. Oxidation Potential (E^0_{ox}) of ArOH and the Rate Constants for the C−C Coupling Reactions of ArOH by the (μ-η^2:η^2-Peroxo)dicopper(II) Complex (**A**), the Bis(μ-oxo)dicopper(III) Complex (**B**), and Cumylperoxyl Radical (**C**)

	ArOH	E^0_{ox} / V [a] (*vs.* SCE)	k_2 / M^{-1} s^{-1} A [b]	B [c]	C
1	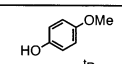	1.43	16.6	—— [d]	70
2	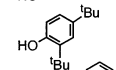	1.46	3.84	—— [d]	28
3	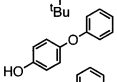	1.49	1.51	41.4	8.6
4	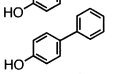	1.52	0.36	15.1	8.3
5	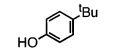	1.52	0.22	13.1	9.0
6	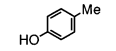	1.54	0.17	7.5	11
7	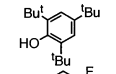	1.58	0.015	0.47	61
8	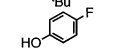	1.61	0.0077	0.30	—— [e]
9	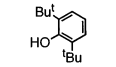	1.62	0.0040	0.18	17
10	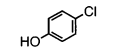	1.63	0.0026	0.10	—— [e]

[a] Determined by SHACV in CH_3CN at 25 °C. [b] $[Cu^{II}_2(L^{Py2})_2(\mu\text{-}O_2)]^{2+}$ (7.5×10^{-5} M) in acetone at −80 °C. [c] $[Cu^{III}_2(L^{Py1})_2(\mu\text{-}O)_2]^{2+}$ (7.5×10^{-5} M) in acetone at −80 °C. [d] Too fast to be determined. [e] Too slow to be determined.

The reaction was followed by UV−vis spectrum by monitoring a decrease in absorbance at 364 nm due to the (μ-η^2:η^2-peroxo)dicopper(II) complex (**A**) (Figure 1). The reaction obeyed first-order kinetics in the presence of an excess amount of the substrate (see inset of Figure 1), and the pseudo-first-order rate constant k_{obs} was proportional to the substrate concentration as demonstrated in Figure 2, from which the second-order rate constant k^A_2 was obtained as the slope. These

(21) The phenol-oxidation reactions by the Cu_2/O_2 complexes were carried out under anaerobic conditions (an excess amount of O_2 was removed by bubbling Ar gas after the generation of Cu_2/O_2 complexes) at −80 °C for several hours, and the reaction mixtures were quenched at this temperature (−80 °C) by adding $HClO_4$ (see Experimental Section). In all the cases examined, the dimer products of phenols were obtained as solely isolable products in less than 50% yields, but neither the corresponding catechols nor the quinone products were obtained from the final reaction mixtures. Thus, the Cu_2/O_2 complexes act as one-electron oxidants rather than two-electron oxidants, when the reduced Cu_2/O_2 complexes produced in the oxidation of phenol may have no ability to further oxidize the phenol. However, the reactivity of the reduced Cu_2/O_2 complexes has yet to be clarified.

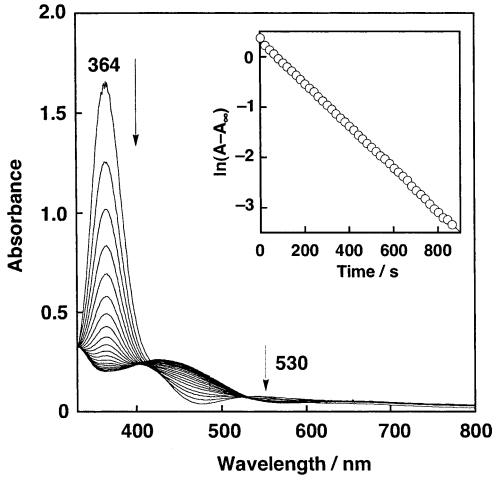

Figure 1. Spectral change for the reaction of 4-*tert*-butylphenol (20×10^{-3} M) and $[Cu^{II}_2(L^{Py2})_2(\mu\text{-}O_2)]^{2+}$ (**A**) (7.5×10^{-5} M) in acetone at −80 °C. Interval: 60 s. Inset: Pseudo-first-order plot based on the absorption change at 364 nm.

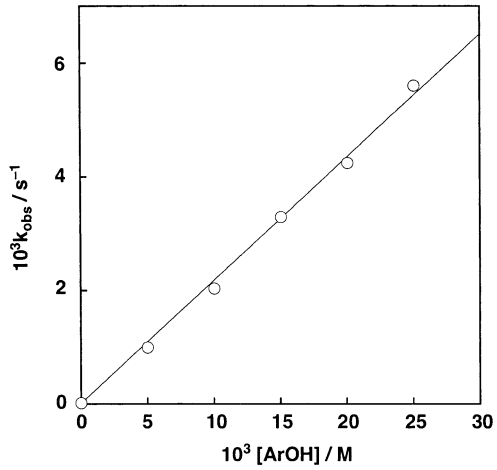

Figure 2. Plot of k_{obs} against the substrate concentration for the reaction between 4-*tert*-butylphenol and $[Cu^{II}_2(L^{Py2})_2(\mu\text{-}O_2)]^{2+}$ (**A**) in acetone at −80 °C.

kinetic behaviors indicate that the reaction between the neutral phenol and peroxo complex **A** is a simple bimolecular process in contrast to the case of oxygenation reaction of the lithium phenolate by **A** (Scheme 1), where a Michaelis−Menten type saturation dependence of the rate on the substrate concentration was observed.[9] The second-order rate constants k^A_2 for the oxidation of variously substituted phenols by **A** were determined similarly and are listed in Table 1 together with the E^0_{ox} values of the phenols determined using the second-harmonic ac voltammetry (SHACV) (S1).[22]

The k^A_2 values of the phenols increase with increasing the driving force of electron transfer from phenols to **A**, i.e., with decreasing the E^0_{ox} values. According to the Marcus theory of electron transfer, a plot of $(RT/F)\ln k$ vs the free energy change of electron transfer (ΔG^0_{et}), which is given by ($E^0_{ox} - E^0_{red}$), should be linear with a slope of −0.5, provided that the driving force of electron transfer ($-\Delta G^0_{et}$) is much smaller than the reorganization energy of electron transfer (λ).[23] Plot of (RT/F)-

(22) The SHACV has been demonstrated to provide a superior approach to directly evaluating the one-electron redox potentials in the presence of a follow-up chemical reaction, relative to the better-known dc and fundamental harmonic ac methods. See: Patz, M.; Mayr, H.; Maruta, J.; Fukuzumi, S. *Angew. Chem., Int. Ed. Engl.* **1995**, *34*, 1225−1227.

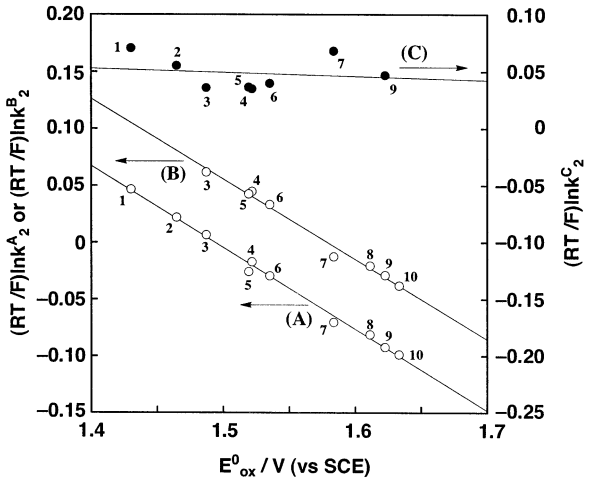

Figure 3. Plots of $(RT/F)\ln(k_2)$ against the oxidation potential (E^0_{ox}) of ArOH for the reactions of ArOH with (μ-η^2:η^2-peroxo)dicopper(II) complex (**A**), bis(μ-oxo)dicopper(III) complex (**B**), and cumylperoxyl radical (**C**) in acetone at −80 °C.

Scheme 2

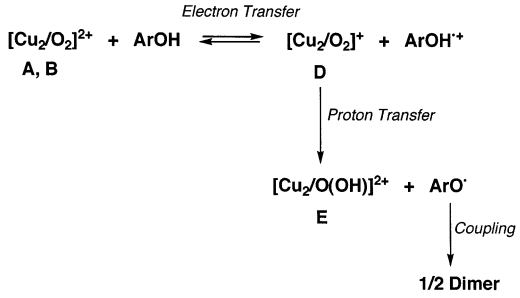

ln k^A_2 vs E^0_{ox} for the one-electron oxidation of phenols by **A** affords good linear correlations as expected for electron-transfer reactions (part A in Figure 3). However, the slope (−0.72) is significantly more negative than −0.5.

The electron transfer from ArOH to **A** may be followed by proton transfer from the resulting cation radical intermediate $ArOH^{\bullet+}$ to an intermediate **D** $[Cu_2/O_2]^+$ to generate a phenoxyl radical species $ArO^\bullet$ and the product complex **E** $[Cu_2/O(OH)]^{2+}$ (Scheme 2).[24] For the intermediates **D**, a (μ-oxo)(μ-oxyl radical)-dicopper(II) or a bis(μ-oxo)dicopper(II,III) form can be drawn. The phenoxyl radical species $ArO^\bullet$ thus produced readily coupled to give the C−C coupling dimer product in ∼50% based on **A** as experimentally observed.[25]

If electron transfer from phenols to the peroxo complex **A** is the rate-determining, followed by the fast proton transfer, the slope of the Marcus plot in Figure 3 (part A) should be the normal value of −0.5, when the electron transfer is exergonic (the free energy change of electron transfer is negative).[23] On the other hand, if the proton transfer is the rate-determining,

(23) Marcus, R. A.; Sutin, N. *Biochim. Biophys. Acta* **1985**, *811*, 265−322.

(24) The intermediate **E** $[Cu_2/O(OH)]^{2+}$ might have a structure of (μ-oxo)(μ-hydroxo)dicopper(II,III) or (μ-oxyl radical)(μ-hydroxo)dicopper(II,II). Thus **E** must be ESR active. However, the ESR spectrum of the final reaction mixture was essentially ESR silent with a little contamination of a copper-(II) signal ($g_{||} = 2.074$, $g_\perp = 2.059$, $A_{||} = 149$ G). Thus, the intermediate **E** might be further converted into a diamagnetic species such as a tetranuclear copper complex. Further characterization of the product complex has been unsuccessful due to its instability at higher temperature.

(25) In the case of 2,4,6-tri-*tert*-butylphenol (**7**), formation of the corresponding phenoxyl radical ($ArO^\bullet$, $\lambda_{max} = 400$, 630 nm) was confirmed by the UV−vis spectrum. For spectral data of $ArO^\bullet$, see: Forrester, A. R.; Hay, J. M.; Thomson, R. H. *Organic Chemistry of Stable Free Radicals*; Academic: New York, 1968; pp 1−80.

the electron transfer is in equilibrium and thereby the slope should be −1.0, when the free energy of electron transfer is normally endergonic (the free energy of electron transfer is positive).[23] If the rates of electron transfer and proton transfer are comparable and thereby coupled to each other, a value between −0.5 and −1.0 would be obtained.[26,27] Thus, the slope of −0.72 observed in Figure 3 (part A) indicates that the electron transfer from phenols to **A** is endergonic and coupled with the proton transfer (PCET mechanism) as illustrated in Scheme 2.

Kinetic deuterium isotope effects on the second-order rate constants k^A_2 ($k^A_{2(H)}/k^A_{2(D)}$) were determined as 1.32 for phenol **1** [*p*-$MeOC_6H_4OH(D)$], 1.23 for phenol **3** [*p*-$PhOC_6H_4OH(D)$], 1.56 for phenol **5** [*p*-$Bu^tC_6H_4OH(D)$], and 1.21 for phenol **10** [*p*-$ClC_6H_4OH(D)$]. Existence of the distinct kinetic deuterium isotope effects (1.21−1.56) clearly indicates that the proton transfer is involved in the rate-determining step. These values are, however, significantly small as compared to the kinetic deuterium isotope effects observed in the hydrogen atom transfer reaction (HAT) from toluene and dihydroanthracene to permanganate ($k_H/k_D = 6 \pm 1$ and 3.0 ± 0.6, respectively),[28] but are nearly the same to that reported for the proton-coupled electron-transfer reaction (PCET) between guanine and $Ru(bpy)_3^{3+}$ ($k_H/k_D = 1.4$).[26b] These results strongly support the PCET mechanism for the oxidation of phenols by the peroxo complex **A**. Recent DFT studies by Mayer and coworkers have suggested that PCET mechanism is more likely than the HAT mechanism for the oxidation of a phenol to a phenoxyl radical species.[29]

Oxidation of Phenols by the Bis(*μ*-oxo)dicopper(III) Complex (B). Oxidation of phenols by the bis(*μ*-oxo)dicopper(III) complex **B** was also examined under the same experimental conditions (at −80 °C in acetone, anaerobic). The bis(*μ*-oxo)dicopper(III) complex was generated by the reaction of the copper(I) complex of the didentate ligand L^{Py1} and O_2. In this case as well, the oxidation product was the corresponding C−C coupling dimers as reported previously,[7a] and the yields were determined as 45%, 42%, and 37% for the dimer products from *p*-$MeOC_6H_4OH$ (**1**), *p*-$Bu^tC_6H_4OH$ (**5**), and *p*-ClC_6H_4OH (**10**), respectively. In this case as well, the lower yield of **10** can be attributed to the lower reactivity of **10** toward the bis(*μ*-oxo) complex **B**. Thus, nearly the same yields around 50% of the dimer products also suggest that the bis(*μ*-oxo)dicopper(III) complex **B** also acts as a one-electron oxidant for the phenol oxidation.[21]

The second-order rate constants k^B_2 have been determined by the same kinetic treatment (first-order dependence both on **B** and the substrate, see Supporting Information S2 and S3). Plot of $(RT/F)\ln k^B_2$ vs E^0_{ox} for the one-electron oxidation of phenols by **B** in Figure 3 (part B) also gives a good linear correlation with virtually the same slope (−0.71) as in the case of **A** (−0.72) in Figure 3 (part A). Kinetic deuterium isotope effects ($k^B_{2(H)}/k^B_{2(D)}$) have also been determined as 1.22 for phenol **3** [*p*-$PhOC_6H_4OH(D)$], 1.48 for phenol **5** [*p*-$Bu^tC_6H_4OH(D)$], and 1.23 for phenol **10** [*p*-$ClC_6H_4OH(D)$]. These results indicate that electron transfer from phenols to **B** is also coupled with the subsequent proton transfer (PCET mechanism) as the case of **A** (Scheme 2).[30]

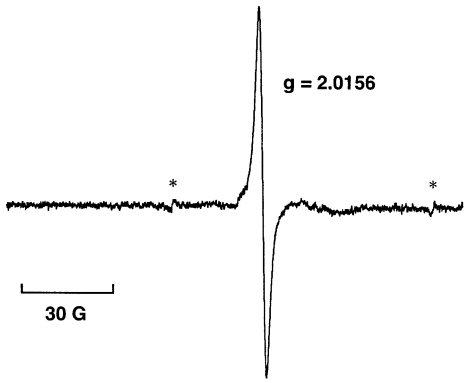

Figure 4. ESR spectrum of cumylperoxyl radical (**C**) in acetone at −80 °C generated in the photoirradiation of an oxygen-saturated acetone solution containing di-*tert*-butyl peroxide (1.0 M) and cumene (1.0 M). The asterisk (*) denotes the Mn^{II} marker.

Oxidation of Phenols by Cumylperoxyl Radical (C). Cumylperoxyl radical has recently been demonstrated to act as a hydrogen atom acceptor in the reaction with *N*,*N*-dimethylanilines, where a one-step hydrogen atom transfer (HAT) mechanism has been confirmed.[31] Thus, the reaction of the same series of phenols with cumylperoxyl radical has also been examined in acetone at −80 °C with use of ESR. Photoirradiation of an oxygen-saturated acetone solution containing di-*tert*-butylperoxide and cumene with a 1000 W Mercury lamp results in formation of the cumylperoxyl radical **C** which was readily detected by ESR as shown in Figure 4. The ESR spectrum consists of a single isotropic signal with the *g* value of 2.0156 showing no detectable hyperfine structure in agreement with the ESR features of cumylperoxyl radical.[32,33]

The cumylperoxyl radical (**C**) is formed via a radical chain process shown in Scheme 3.[34−38] The photoirradiation of Bu^tOOBu^t results in the homolytic cleavage of the O−O bond to produce $Bu^tO^•$,[39,40] which abstracts a hydrogen atom from cumene to give cumyl radical, followed by the facile addition of oxygen to give **C**. The cumylperoxyl radical (**C**) can also abstract a hydrogen atom from cumene in the propagation step

(26) (a) Goto, Y.; Watanabe, Y.; Fukuzumi, S.; Jones, J. P.; Dinnocenzo, J. P. *J. Am. Chem. Soc.* **1998**, *120*, 10762−10763. (b) Weatherly, S. C.; Yang, I. V.; Thorp, H. H. *J. Am. Chem. Soc.* **2001**, *123*, 1236−1237. (c) Ram, M. S.; Hupp, J. T. *J. Phys. Chem.* **1990**, *94*, 2378−2380.
(27) The precise dependence expected would be a curved plot with a limiting slope of −0.5 at low driving forces and a limiting slope of −1.0 at high driving forces. The range of driving forces investigated here likely does not allow this dependence to be resolved, resulting in a linear plot with an overall slope of −0.72.
(28) Gardner, K. A.; Kuehnert, L. L.; Mayer, J. M. *Inorg. Chem.* **1997**, *36*, 2069−2078.
(29) Mayer, J. M.; Hrovat, D. A.; Thomas, J. L.; Borden, W. T. *J. Am. Chem. Soc.* **2002**, *124*, 11142−11147.
(30) Tolman and co-workers have demonstrated an important role of hydrogen bonding interaction between the oxygen atom of bis(*μ*-oxo)dicopper(III) core and a hydrogen atom being activated in the aliphatic ligand hydroxylation reaction: Mahapatra, S.; Halfen, J. A.; Wilkinson, E. C.; Pan, G.; Wang, X.; Young, V. G., Jr.; Cramer, C. J.; Que, L., Jr.; Tolman, W. B. *J. Am. Chem. Soc.* **1996**, *118*, 11555−11574. Such a hydrogen bonding interaction between the oxo group of **B** and phenols may also play an important role to accelerate the electron-transfer step.
(31) Fukuzumi, S.; Shimoosako, K.; Suenobu, T.; Watanabe, Y. *J. Am. Chem. Soc.* **2003**, *125*, 9074−9082.
(32) Bersohn, M.; Thomas, J. R. *J. Am. Chem. Soc.* **1964**, *86*, 959.
(33) Fukuzumi, S.; Ono, Y. *J. Chem. Soc., Perkin Trans. 2*. **1977**, 622−625.
(34) Sheldon, R. A. In *The Activation of Dioxygen and Homogeneous Catalytic Oxidation*; Barton, D. H. R., Martell, A. E., Sawyer, D. T., Eds.; Plenum: New York and London, 1993; pp 9−30.
(35) Parshall, G. W.; Ittel, S. D. *Homogeneous Catalysis*, 2nd ed.; Wiley: New York, 1992; Chapter 10.
(36) Sheldon, R. A.; Kochi, J. K. *Adv. Catal.* **1976**, *25*, 272−413.
(37) Shilov, A. E. *Activation of Saturated Hydrocarbons by Transition Metal Complexes*; D. Reidel Publishing Co.: Dordrecht, The Netherlands, 1984; Chapter 4.
(38) Bottcher, A.; Birnbaum, E. R.; Day, M. W.; Gray, H. B.; Grinstaff, M. W.; Labinger, J. A. *J. Mol. Catal.* **1997**, *117*, 229−242.
(39) Kochi, J. K. *Free Radicals in Solution*; J. Wiley & Sons: New York, 1957.

Scheme 3

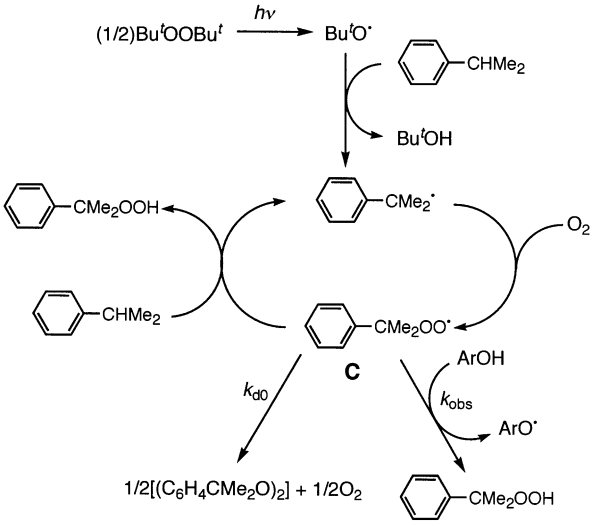

to yield cumene hydroperoxide, accompanied by regeneration of cumyl radical (Scheme 1).[33,41] In the termination step, cumylperoxyl radicals decay by a bimolecular reaction to yield the corresponding peroxide and oxygen (Scheme 3).[33,41] When the light is cut off, the ESR signal intensity decays obeying second-order kinetics due to the bimolecular reaction in Scheme 3 ([**5**] = 0 M in Figure 5a).[42]

In the presence of ArOH, the decay rate of **C** after cutting off the light becomes much faster than that in the absence of ArOH as shown in Figure 5a. The decay rate in the presence of ArOH obeys pseudo-first-order kinetics rather than second-order kinetics as shown in Figure 5b. Thus, the decay of the ESR signal due to **C** in the presence of ArOH is ascribed to the hydrogen atom transfer from ArOH to **C** (Scheme 3). The pseudo-first-order rate constants (k_{obs}) increase linearly with an increase in [ArOH] as shown in Figure 6. The rate constants (k^C_2) of intermolecular hydrogen atom transfer from a series of ArOH to **C** are determined from the slope of linear plots (Figure 6), and the determined k^C_2 values are listed in Table 1.

Plot of (RT/F)ln k^C_2 vs E^0_{ox} for the net-hydrogen atom transfer from ArOH to cumylperoxyl radical is shown in Figure 3 (part C), where the k^C_2 values are rather constant irrespective of the E^0_{ox} values. The small rate-dependence of k^C_2 on E^0_{ox} is similar to the case of the HAT reaction with *N*,*N*-dimethylanilines,[31] but shows sharp contrast with the case of the one-electron oxidation of ArOH by the Cu_2/O_2 complexes in Figure 3 (parts A and B). The contrasting results in Figure 3 (parts A and B vs part C) confirm that the electron transfer step is definitely involved in the oxidation of phenols by (μ-η^2:η^2-peroxo)dicopper(II) complex (**A**) and the bis(μ-oxo)dicopper(III) complex (**B**).

Reactive Cu_2/O_2 Species in the Phenol-Oxidation. So far, oxidation reactions of phenols by the (μ-η^2:η^2-peroxo)dicopper(II) complex (**A**) and the bis(μ-oxo)dicopper(III) complex (**B**) have been investigated to demonstrate that the yield of C−C coupling dimer and the dependence of k_2 on E^0_{ox} (Figure 3) as well as the kinetic deuterium isotope effect ($k_{2(H)}/k_{2(D)}$) were nearly the same between the two systems. The only difference was found in the rate constants, k^A_2 vs k^B_2, for the same substrate; the k^B_2 values are about two-order of magnitude larger than the k^A_2 values (Table 1). These differences in the rate constants could be attributed to the difference in the intrinsic reactivity between the peroxo complex **A** and the bis(μ-oxo)

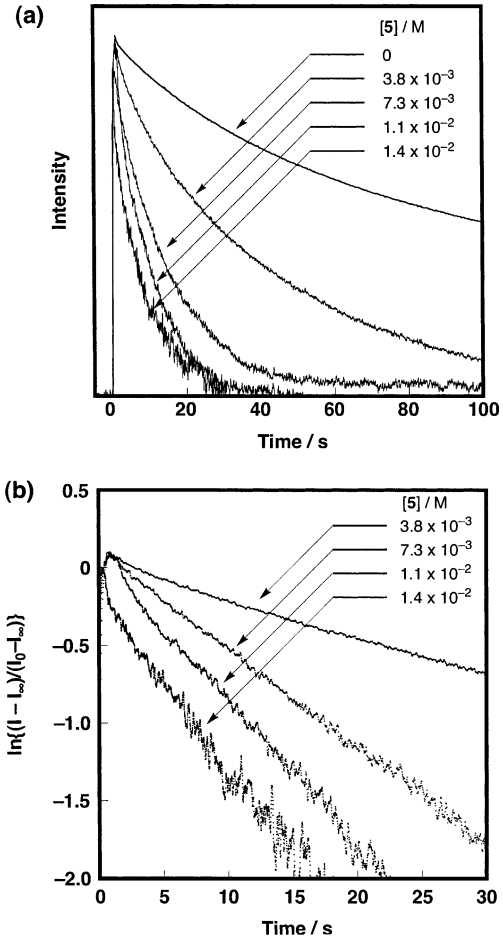

Figure 5. (a) Time dependence of the ESR signal intensity of cumylperoxyl radical (**C**) in the presence of **5** in O_2-saturated acetone at −80 °C. (b) First-order plots.

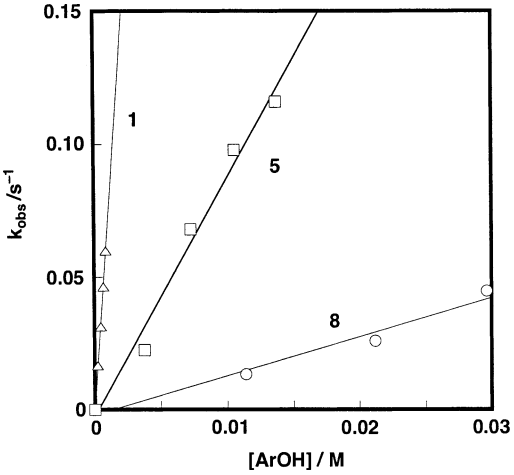

Figure 6. Plots of k_{obs} vs [ArOH] for hydrogen transfer from ArOH (**1**, **5**, and **8**) to cumylperoxyl radical (**C**) in O_2-saturated acetone at −80 °C.

(40) (a) Kochi, J. K.; Krusic, P. J.; Eaton, D. R. *J. Am. Chem. Soc.* **1969**, *91*, 1877−1879. (b) Krusic, P. J.; Kochi, J. K. *J. Am. Chem. Soc.* **1968**, *90*, 7155−7157. (c) Kochi, J. K.; Krusic, P. J. *J. Am. Chem. Soc.* **1969**, *91*, 3938−3940. (d) Kochi, J. K.; Krusic, P. J. *J. Am. Chem. Soc.* **1969**, *91*, 3942−3944. (e) Kochi, J. K.; Krusic, P. J. *J. Am. Chem. Soc.* **1969**, *91*, 3944−3946. (f) Howard, J. A.; Furimsky, E. *Can. J. Chem.* **1974**, *52*, 555−556.
(41) Fukuzumi, S.; Ono, Y. *J. Chem. Soc., Perkin Trans. 2* **1977**, 784−788.
(42) Howard, J. A. *Adv. Free-Radical Chem.* **1972**, *4*, 49−173.

complex **B** for the oxidation of ArOH. In such a case, the one-electron reduction potential (E^0_{red}) of **B** may be ~0.1 V higher than the E^0_{red} value of **A** judging from the two parallel relations in Figure 3.

There is, however, another possibility that the bis(μ-oxo) complex **B** is the real active species in both cases, and the rate difference between the two systems is attributed to the difference in absolute concentration of **B**. Namely, in the tridentate ligand system L^{Py2}, the peroxo complex **A** is the major species and the bis(μ-oxo) complex **B** exists as a minor component in the rapid equilibrium between them. In such a case, the observed rate constant is given as $k^B{}_2K/(1 + K)$, where K is an equilibrium constant between **A** and **B** in the tridentate ligand system. Then, the K value is estimated as $0.017 - 0.037$, given that the $k^B{}_2$ value in the tridentate ligand system L^{Py2} is the same to the $k^B{}_2$ value in the didentate ligand system L^{Py1}. This is consistent with the previous report that the bis(μ-oxo)dicopper(III) complex coexists as a minor product when the (μ-η^2:η^2-peroxo)dicopper-(II) complex is prepared using 2-(2-pyridyl)ethylamine tridentate ligands $(PyCH_2CH_2)_2NR$.[43,44]

If the peroxo complex **A** was a real active species for PCET-oxidation of neutral phenols, the reaction of **A** with lithium phenolate would proceed via an outer sphere electron-transfer mechanism, since the phenolate has a much more negative oxidation potential than the corresponding neutral phenol. In such a case, the oxidation product of lithium phenolate by the peroxo complex **A** should also be the phenoxyl radical which is eventually converted into the dimer product. This is, however, inconsistent with the previous data demonstrating that the oxygenation of phenolate by the peroxo complex **A** proceeds via the electrophilic aromatic substitution mechanism in an association complex to give the catechols, but not the dimer, as shown in Scheme 1. Thus, the bis(μ-oxo)dicopper(III) complex (**B**) may be the real active species in both the tridentate and didentate ligand systems, and the reduction potential of (μ-η^2:η^2-peroxo)dicopper(II) complex (**A**) may be much more negative than that of **B**. This may be the reason tyrosinase employs the (μ-η^2:η^2-peroxo)dicopper(II) intermediate to accomplish the aromatic oxygenation reaction of phenols. In other words, formation of a phenoxyl radical species by the reaction of a phenol substrate with the bis(μ-oxo)dicopper(III) intermediate may be prevented in the enzymatic system by keeping the Cu−Cu distance about 3.5 Å, which can only accommodate the (μ-η^2:η^2-peroxo)dicopper(II) intermediate.[45]

Acknowledgment. This work was financially supported in part by Grants-in-Aid for Scientific Research on Priority Area (No. 11228206) and Grants-in-Aid for Scientific Research (No. 13480189 and 15350105) from the Ministry of Education, Culture, Sports, Science and Technology, Japan.

Supporting Information Available: The SHACV data of phenol **5** (S1) and the kinetic data of complex **B** (S2, S3). This material is available free of charge via the Internet at http://pubs.acs.org.

JA029380+

(43) Pidcock, E.; DeBeer, S.; Obias, H. V.; Hedman, B.; Hodgson, K. O.; Karlin, K. D.; Solomon, E. I. *J. Am. Chem. Soc.* **1999**, *121*, 1870−1878.

(44) The equilibrium position between **A** and **B** has been suggested to be largely dependent on the size of the alkyl group R in the tridentate ligand $(PyCH_2CH_2)_2NR$.[17b] When R is a small substituent such as methyl, the content of **B** becomes larger (~20%),[43] but the population of **B** in the equilibrium becomes significantly smaller when R is larger such as benzyl and phenethyl; Itoh, S.; Nakao, H.; Berreau, L. M.; Kondo, T.; Komatsu, M.; Fukuzumi, S. *J. Am. Chem. Soc*. **1998**, *120*, 2890−2899.

(45) The bis(μ-oxo)dicopper(III) complex requires much shorter Cu−Cu distance (~2.8 Å).[14]